Influence of Silver on the Structural, Optical and Gas-Sensing Properties of Nickel Oxide Nanostructures Thin Films

Esraa Hassn Hadi[1], Ali Mohammed Jabbar[2], Mushtak Abdulmohsen Jabbar[1], Wathiq Ayoub Taha Al Ramdhan[3], Ali Taher Mohi[1] and Muhannad Jadan[4]
[1]Department of Physics, College of Education, Mustansiriyah University, 10052 Baghdad, Iraq
[2]Department of Physics, College of Science, Mustansiriyah University, 10052 Baghdad, Iraq
[3]Department of Medical Physics, Al-Manara College for Medical Sciences, 62001 Amarah, Maysan, Iraq
[4]Department of Applied Physics, Faculty of Science, Tafila Technical University, PO Box 179, 66110 Tafila, Jordan
dr.alitaher@uomustansiriyah.edu.iq

Keywords: NiO, Ag Doping, Thin Films, CSP, XRD, AFM, Optical Properties, Gas Sensor.

Abstract: In this study, undoped and silver (Ag)-doped nickel oxide (NiO) thin films were successfully grown by chemical spray pyrolysis (CSP) technique. XRD revealed that all films are polycrystalline, exhibiting a preferred orientation along the (200) plane. The crystallite size increased from 15.62 nm to 24.47 nm with increasing Ag content, accompanied by a reduction in microstrain and dislocation density, indicating improved crystallinity. Atomic force microscopy (AFM) images showed a decrease in average particle size from 78.3 nm to 41.1 nm and a reduction in surface roughness upon Ag doping, suggesting a more homogeneous, compact surface morphology. Optical transmittance measurements indicated a slight reduction in transparency from 72.8% to 68.9% with doping. The bandgap decreased from 3.56 eV to 3.43 eV. The refractive index and extinction coefficient decreased via Ag concentration, reflecting changes in the electronic polarizability and absorption behaviour. Gas-sensing measurements demonstrated that Ag doping significantly reduced the sensitivity to NH_3, with values decreasing from 48.96% for undoped NiO to 20.28% for 3% Ag-doped films at 300 ppm.

1 INTRODUCTION

NiO is a wide-bandgap (3.6-4.0 eV) transition-metal oxide semiconductor that has attracted considerable interest in diverse technological applications, particularly in gas sensing [1]-[4]. NiO exhibits remarkable physical properties, making it appropriate for applications such as supercapacitors and photocatalysis [5]-[8]. Its technological importance is further enhanced by its low cost, non-toxicity, and favorable physicochemical properties [9], [10]. The performance of NiO-based devices is strongly governed by their structural, morphological, and electronic characteristics, which can be effectively tailored through doping with foreign elements [11], [12]. Doping induces lattice distortions, modifies charge carrier concentration, and introduces defect states within the band structure, thereby enabling precise tuning of material properties for targeted applications [13], [14]. Various methods were employed for the fabrication of NiO thin films, like CBD [15], PLD [16], beam sputtering [17], RF sputtering [18], PECVD [19] and CSP [20]-[22]. CSP is a simple, cost-effective, and scalable deposition method suitable for large-area thin-film production [23], [24]. The present work aims to systematically synthesize undoped and Ag-doped NiO thin films (1% and 3%) using the CSP technique to study structural properties, surface parameters, and ultimately the selective gas sensing performance toward NH_3.

2 EXPERIMENTAL

The precursor solution was prepared by dissolving 0.05 M of ($Ni(CH_3COO)_2 \cdot xH_2O$) in 100 mL of DI water to obtain a homogeneous aqueous solution. A dopant solution was prepared by dissolving 0.1 M silver nitrate hydrate ($AgNO_3 \cdot xH_2O$) in DI water. This solution was then incorporated into the precursor to achieve doping concentrations of 1% and 3% by volume. The deposition parameters were optimized at a base temperature of 400 °C. The distance between base and the spray nozzle was maintained at 29 cm, the spray duration was set to 8 s, and the interval between successive spray cycles was 1.5 min. The film thickness was determined using the weighing method, yielding an average thickness of approximately (330 ± 25) nm. Transmittance spectra were computed via a Shimadzu UV-Probe 1650 Japan. XRD estimated the structural properties, and the surface morphology was examined using AFM. Gas-sensitivity measurements were conducted in a cylindrical chamber with a 9 cm radius and an 18 cm height.

3 RESULTS AND DISCUSSION

Figure 1 illustrates XRD patterns of the deposited films. The observed diffraction peaks at 2θ = 37.26° and 43.89° are indexed to the (111) and (200) planes, respectively, corresponding to orthorhombic NiO in accordance with ICDD card No. 75-0197, confirming the polycrystalline nature of the deposited films. The preferred orientation along the (200) plane remains dominant across all samples, regardless of Ag doping concentration [25], indicating that the fundamental crystal growth mechanism is not significantly altered by Ag incorporation. This preferential growth can be attributed to the lower surface energy of the (200) plane, which makes it thermodynamically more stable during film formation [26].

The crystallite size (D) was computed from the diffraction peak's FWHM (β) and the X-ray wavelength (λ = 1.5406 Å) using the Scherrer equation [27], [28].

Table 1 summarizes the computed D values corresponding to the (200) plane. The results reveal a systematic increase in D with increasing Ag content, with values ranging from 15.62 to 24.47 nm. This trend is attributable to the enhancement of crystal growth and the reduction in lattice imperfections upon Ag incorporation, which facilitate grain coalescence and improve crystallinity [29].

Furthermore, the strain (ε), which reflects lattice distortions within the crystallites, was estimated using the standard relation between the diffraction peak broadening and the Bragg angle [30], [31].

As presented in Table 1, ε in NiO thin films decreases systematically from 21.62×10^{-4} for the undoped sample to 14.26×10^{-4} for the 3% Ag-doped films (Fig. 6). This reduction in strain indicates a progressive relaxation of lattice distortions with increasing Ag incorporation, which is generally associated with improved crystallinity and enhanced structural ordering within the film matrix. The decrease in microstrain can be explained by the partial accommodation of dopant ions within the NiO lattice, which reduces local lattice imperfections and relieves internal stress generated during film growth [32], [33].

The dislocation density (δ), which is inversely related to the square of the crystallite size, was calculated following [34].

The dislocation density decreases from 30.48×10^{14} lines/m² for the undoped sample to 15.51×10^{14} lines/m² for the film doped with 3% Ag. This reduction suggests an improvement in crystalline quality with increasing Ag content, as a lower dislocation density corresponds to fewer structural defects in the lattice [35]. Figure 2 shows the variation of FWHM, D, δ, and ε with respect to Ag doping, illustrating the effect of dopant content on the crystalline structure of the NiO films.

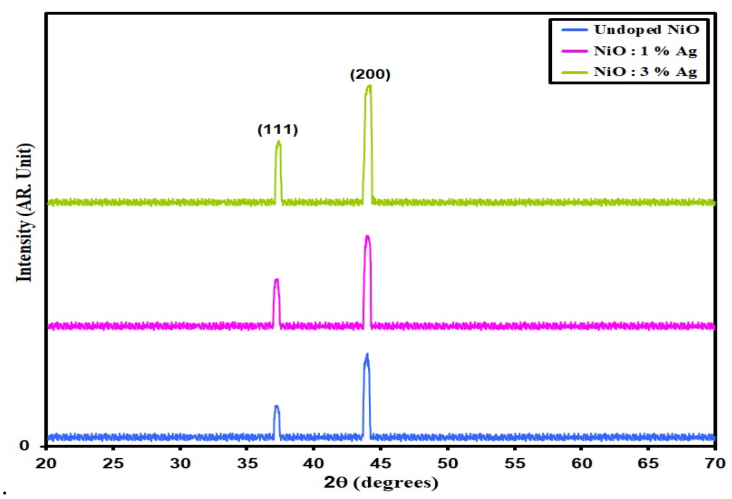

Figure 1: XRD patterns of undoped and Ag-doped NiO thin films.

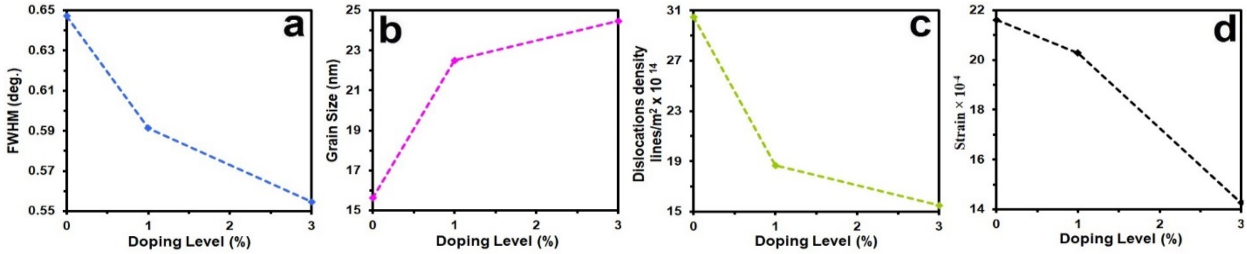

Figure 2: Variation of structural parameters (FWHM, crystallite size, dislocation density, and microstrain) of Ag-doped NiO thin film.

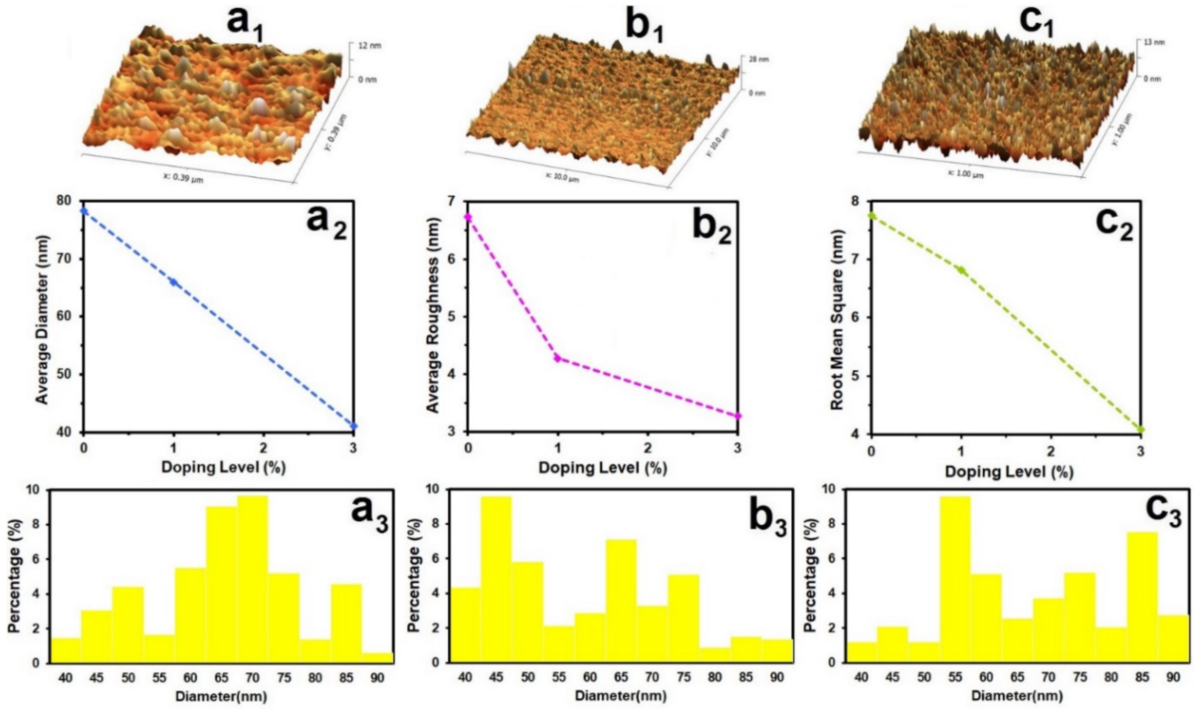

Figure 3: AFM surface morphology images of undoped and Ag-doped NiO thin films.

Table 1: Structural parameters and optical band gap energy of undoped and Ag-doped NiO thin films.

Sample	(hkl) Plane	2 θ (°)	FWHM (°)	E_g (eV)	*D* (nm)	δ (× 10^{14}) (lines/m^2)	*E* × 10^{-4}
Undoped NiO	200	37.26	0.65	3.56	15.62	30.48	21.62
NiO: 1% Ag	200	37.23	0.59	3.50	22.50	18.68	20.28
NiO: 3%Ag	200	37.20	0.55	3.43	24.47	15.51	14.26

Table 2: AFM surface parameters of undoped and Ag-doped NiO thin films.

Sample	P_{av} (nm)	R_a (nm)	RMS (nm)
Undoped NiO	78.3	6.73	7.75
NiO: 1% Ag	66.0	4.27	6.82
NiO: 3% Ag	41.1	3.28	4.08

Figure 3 presents the AFM images of undoped NiO and Ag-doped NiO samples. The average particle size (P_{av}) and root mean square (RMS) roughness values were found to be 78.3, 66.0, and 41.1 nm, and 7.75, 6.82, and 4.08 nm for undoped NiO, NiO:1% Ag, and NiO:3% Ag, respectively. In addition, the surface roughness (R_a)was reduced from 6.73 nm for the undoped sample to 3.27 nm for the 3% Ag-doped film with increasing dopant concentration [36], [37]. The AFM parameters (P_{AFM}) are summarized in Table 2. This systematic decrease in P_{av} and surface roughness with increasing Ag content can be explained by the impact of Ag incorporation on the nucleation and growth dynamics of the NiO thin films. Specifically, the presence of dopant ions modifies the surface diffusion processes and inhibits excessive grain coalescence, leading to the formation of finer and more uniformly distributed grains. Consequently, a smoother and more homogeneous surface morphology is obtained at higher doping levels [38], [39].The transmittance (T) was determined from the ratio of the transmitted light intensity (I) to the incident light intensity (I_0) [40].

The optical transmittance (T) spectra are illustrated in Figure 4. Undoped NiO thin film exhibits a high transparency of 72.8%, while the Ag-doped NiO film with 3% Ag concentration shows a slightly reduced transmittance of 68.9%. This decrease in optical transparency with increasing Ag content is attributable to enhanced light scattering and increased free carrier absorption induced by dopant incorporation, as well as the possible introduction of defect states within the band structure, which collectively contribute to higher optical attenuation in the visible region [41].

The absorption coefficient (α) was determined from the transmittance (T) and film thickness (t) using the following relation [42].

As illustrated in Figure 5, the relatively high values of the absorption coefficient ($\geq 10^{-4}$ cm^{-1}) indicate strong optical absorption and efficient direct electronic transitions within the NiO thin films [43], [44]. The observed rise in α with Ag incorporation suggests an enhancement in photon absorption efficiency, which can be attributed to improved light-matter interaction and increased carrier concentration [44], [45].

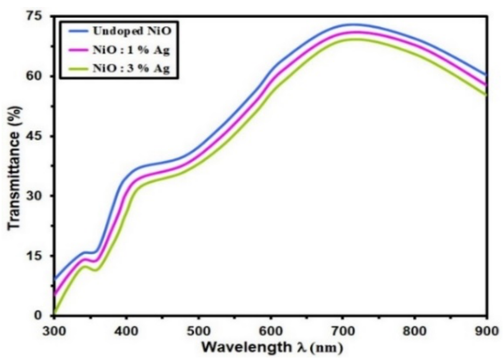

Figure 4: Optical transmittance spectra of undoped and Ag-doped NiO thin films with different Ag concentrations.

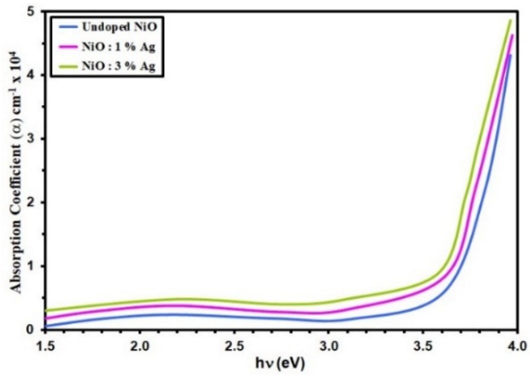

Figure 5: Absorption coefficient spectra of undoped and Ag-doped NiO thin films.

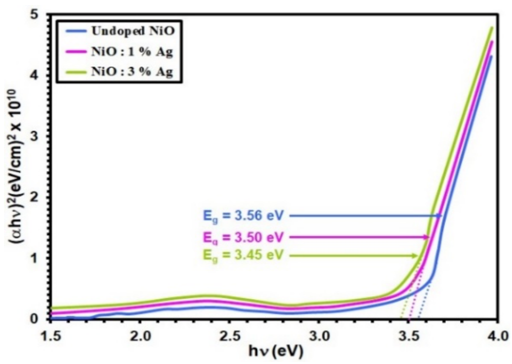

Figure 6: Optical band gap energy of undoped and Ag-doped NiO thin films.

The extinction coefficient (k) was computed from the absorption coefficient (α) and wavelength (λ) [46].

Figure 7 shows k as a function of λ. k decreased with increasing Ag content, establishing that films absorb less light as Ag doping rises [47], [48]. Differences in the electronic structure and a lower density of accessible states for photon absorption are responsible for this behavior [49], [50].

The refractive index (n) was computed from the reflectance (R) of the film and the extinction coefficient (k) [51].

Figure 8 shows the variation of n with wavelength for the NiO films. It is observed that all NiO:Ag films exhibit a refractive index that varies systematically with wavelength, showing a clear dependence on the optical dispersion behavior of the material. In addition, n increases with increasing Ag content [52], [53]. This trend is attributable to the alteration of the film's electronic polarizability and density due to Ag incorporation [54], [55].

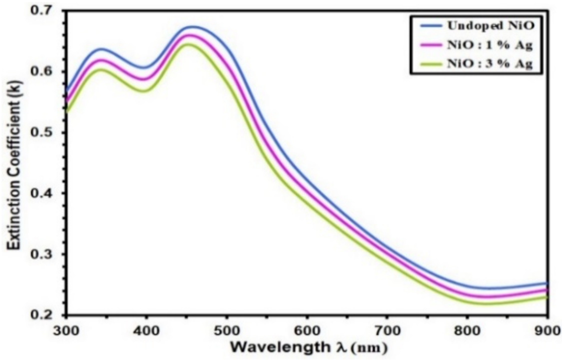

Figure 7: Extinction coefficient spectra of undoped and Ag-doped NiO thin films.

The detection sensitivity, often referred to as the sensor response, was determined from the relative change in resistance upon gas exposure, where Ra and Rg represent the sensor's resistance in air and in the presence of gas, respectively [56].

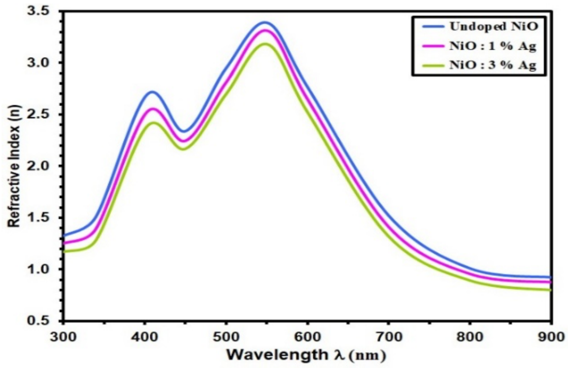

Figure 8: Refractive index spectra of undoped and Ag-doped NiO thin films.

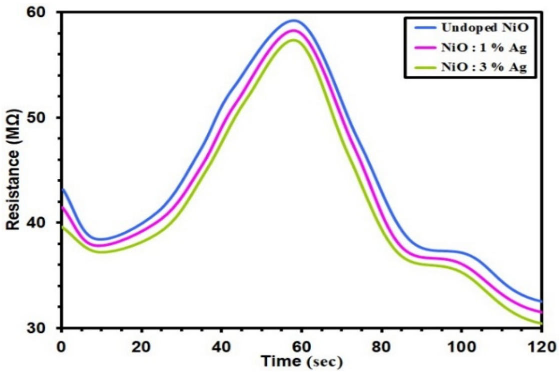

Figure 9: Resistance response of undoped and Ag-doped NiO thin films under NH_3 gas exposure..

The gas sensor fabricated using porous silicon coated with undoped NiO on a glass substrate was tested under exposure to 300 ppm of NH_3 gas. Figure 9 illustrates the resistance-time response for both undoped and Ag-doped NiO thin films at an operating temperature of 150 °C. Upon exposure to NH_3, surface redox reactions occur between the gas molecules and adsorbed oxygen species, leading to the release of electrons from chemisorbed O_2^- ions back into the conduction band. This process increases the electrical resistance of the NiO films and enhances the potential barrier at grain boundaries, which strongly influences charge transport [57], [58]. Among all investigated samples, the NiO film doped with 3% Ag exhibited the highest resistance response [59]. This behaviour is attributable to increased surface area, the higher density of active adsorption sites, and the improved modulation of charge-carrier concentration induced by Ag incorporation [60], [61].

Figure 10 illustrates that the sensitivity to NH_3 gas decreases with increasing Ag doping in NiO thin films. For different doping levels undoped NiO, NiO:1% Ag, and NiO:3% Ag), the sensitivity shows a systematic reduction, decreasing from 46.75% to 22.91% at 100 ppm, from 47.85% to 21.63% at 200 ppm, and from 48.96% to 20.28% at 300 ppm, this decreasing trend is attributable to the change of the surface electronic structure and active adsorption sites upon Ag incorporation [62], [63].

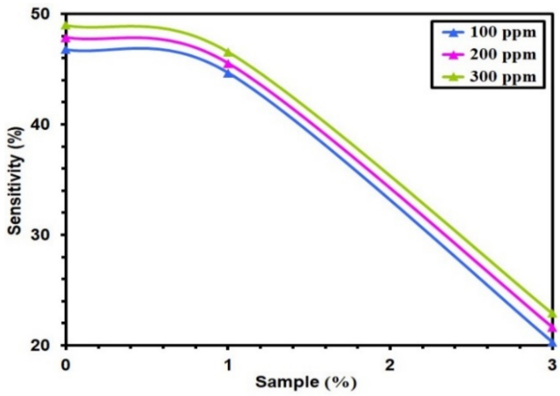

Figure 10: NH_3 gas sensitivity of undoped and Ag-doped NiO thin films.

4 CONCLUSIONS

Undoped and Ag-doped NiO thin films were grown via CSP technique. A comprehensive investigation revealed the significant impact of Ag concentration. XRD analysis confirmed the orthorhombic polycrystalline structure with a dominant (200) orientation. Ag doping led to a systematic increase in crystallite size from 15.62 nm to 24.47 nm, accompanied by a reduction in microstrain from 21.62×10^{-4} to 14.26×10^{-4} and dislocation density from 30.48×10^{14} lines/m² to 15.51×10^{14} lines/m², indicating a significant improvement in crystalline quality. AFM imaging showed that Ag incorporation results in a smoother, more homogeneous surface, with the average particle size decreasing from 78.3 nm to 41.1 nm and the RMS roughness decreasing from 7.75 nm to 4.08 nm. Optically, Ag doping caused a slight reduction in transmittance from 72.8% to 68.9%, a decrease in the bandgap from 3.56 eV to 3.43 eV, an increase in the refractive index, and a decrease in the extinction coefficient. Gas-sensing measurements demonstrated a strong dopant-dependent selectivity: Ag doping significantly enhanced the sensor's response to NH_3. This opposite trend provides a clear pathway for developing highly selective gas sensors by simply controlling the Ag doping level in NiO thin films. Overall, Ag doping is an effective approach to tailor the physical properties of NiO thin films for optoelectronic and selective sensing uses.

ACKNOWLEDGMENTS

The authors gratefully acknowledge the financial and institutional support provided by Mustansiriyah University (www.uomustansiriyah.edu.iq) for this research.

REFERENCES

[1] S. G. Randive, A. V. Kadam, and S. S. Patil, "Morphological tuning of NiO via CSP," Inorganic Chemistry Communications, 2025.

[2] K. Dissanayake, S. Perera, and T. Weerasinghe, "Nickel oxide thin films for energy storage applications," Journal of Energy Storage, vol. 72, 108546, 2023.

[3] U. K. Chime, A. B. C. Ekwealor, and F. I. Ezema, "Recent advances in nickel oxide-based supercapacitors," Current Opinion in Electrochemistry, vol. 21, pp. 123-130, 2020.

[4] X. Tian, X. Wang, and Y. Zhang, "Nickel oxide nanomaterials for gas sensing applications," Nano Materials Science, vol. 3, pp. 390-403, 2021.

[5] N. Baig, M. S. Alghamdi, and H. S. Alghamdi, "Recent progress in nickel oxide-based photocatalysts," Materials Advances, vol. 2, pp. 1821-1871, 2021.

[6] D. Bokov, A. T. Jalil, and M. M. Kadhim, "Nickel oxide thin films: A comprehensive review," Advances in Materials Science and Engineering, vol. 2021, 5102014, 2021.

[7] S. Zhao, Y. Li, and J. Wang, "Structural and optical properties of doped NiO thin films," Journal of Alloys and Compounds, vol. 877, 160189, 2021.

[8] H. Ji, W. Sun, and Y. Li, "Recent advances in NiO-based gas sensors," Nanoscale, vol. 11, pp. 22664-22682, 2019.

[9] N. Goel, K. Kumar, and R. Singh, "Doping engineering of nickel oxide for optoelectronic applications," Engineering Reports, vol. 5, e12604, 2023.

[10] R. Paul, S. Dey, and A. Chakraborty, "Silver-doped nickel oxide thin films: Structure-property correlations," Journal of Alloys and Compounds, vol. 941, 168943, 2023.

[11] M. J. Haque, A. R. Khan, and M. A. Hossain, "Doping effects on NiO thin film properties," Nano Express, vol. 1, 010007, 2020.

[12] Y. C. Liang and Y. C. Chang, "Enhanced optical properties of Ag-doped NiO thin films," CrystEngComm, vol. 22, pp. 2315-2323, 2020.

[13] P. Gupta, S. Sharma, and R. Kumar, "Ag-doped NiO nanostructures for gas sensing applications," Applied Physics A, vol. 127, p. 289, 2021.

[14] T. P. Mokoena, H. C. Swart, and D. E. Motaung, "Doped NiO for gas sensing applications," Journal of Alloys and Compounds, vol. 805, pp. 267-294, 2019.

[15] L. Cattin, B. A. Reguig, A. Khelil, M. Morsli, K. Benchouk, and J. C. Bernede, "Properties of NiO thin films deposited by chemical spray pyrolysis using different precursor solutions," Applied Surface Science, vol. 254, no. 18, pp. 5814-5821, 2008.

[16] I. Hotovq, D. Buc, S. Hascik, and O. Nennewitz, "Characterization of NiO thin films prepared by reactive sputtering," Vacuum, vol. 50, pp. 41-44, 1998.

[17] I. Fasaki, A. Koutoulaki, M. Kompitsas, and C. Charitidis, "Structural, electrical and mechanical properties of NiO thin films grown by pulsed laser deposition," Applied Surface Science, vol. 257, no. 2, pp. 429-433, 2010.

[18] J. Peng, Z. Xu, S. Wang, Q. Jie, and C. Chen, "Preparation and Performance of nickel oxide films by Ion beam sputtering deposition and oxidation annealing," Sensors and Materials, vol. 22, no. 8, pp. 409-416, 2010.

[19] E. Fujii, A. Tomozawa, H. Torii, and R. Takayama, "Preferred orientations of NiO films prepared by plasma-enhanced metalorganic chemical vapor deposition," Japanese Journal of Applied Physics, vol. 35, pp. L328-L330, 1996.

[20] B. A. Reguig, A. Khelil, L. Cattin, M. Morsli, and J. C. Bernede, "Properties of NiO thin films deposited by intermittent spray pyrolysis process," Applied Surface Science, vol. 253, no. 9, pp. 4330-4334, 2007.

[21] S. Sriram and A. Thayumanavan, "Structural, Optical and electrical properties of NiO thin films prepared by low cost spray pyrolysis technique," International Journal of Materials Science and Engineering, vol. 1, no. 2, pp. 118-121, 2013.

[22] R. A. Ismail, S. Ghafori, and G. A. Kadhim, "Preparation and characterization of nanostructured nickel oxide thin films by spray pyrolysis," Applied Nanoscience, vol. 3, pp. 509-514, 2013.

[23] L. N. Bhoye, S. R. Nandurkar, and P. M. Bhujbal, "Synthesis technique influence on NiO gas sensing," Journal of Materials Science: Materials in Electronics, vol. 37, p. 46, 2026.

[24] W. Thongpan, T. Khamman, and S. Maensiri, "Morphological control of NiO for functional devices," Surfaces and Interfaces, vol. 42, 103456, 2023.

[25] K. Zhou, J. Wang, and Y. Zhang, "Surface energy of NiO crystallographic planes," Surfaces and Interfaces, vol. 7, pp. 112-118, 2017.

[26] Y. T. Prabhu, K. V. Rao, and V. S. S. Kumar, "Scherrer equation for crystallite size determination," World Journal of Nano Science and Engineering, vol. 4, pp. 21-28, 2014.

[27] F. S. Ahmed, N. Y. Ahmed, R. S. Ali, N. F. Habubi, K. H. Abass, and S. S. Chiad, "Effects of substrate type on some optical and dispersion properties of sprayed CdO thin films," NeuroQuantology, vol. 18, no. 3, pp. 56-65, 2020.

[28] M. B. Jumaa, T. H. Mubarak, and A. M. Mohammad, "Synthesis and characterization of spinel ferrite Co0.8Fe2.2O4 nanoparticle," Journal of University of Anbar for Pure Science, vol. 15, no. 2, pp. 74-82, 2021.

[29] Y. Fan, H. Zhang, and L. Wang, "Tauc relation for optical bandgap determination," ChemSusChem, vol. 18, e202500462, 2025.

[30] S. S. Chiad, K. H. Abass, T. H. Mubarak, N. F. Habubi, M. K. Mohammed, and A. A. Khadayeir, "Fabrication and study the structure, optical and dispersion parameters of PMMA with InCl3 additive," Journal of Global Pharma Technology, vol. 11, no. 4, pp. 369-375, 2019.

[31] R. S. Sattar, M. A. Rahman, and K. S. Karimov, "Sol-gel synthesis of NiO thin films," Journal of Ovonic Research, vol. 21, pp. 335-342, 2025.

[32] N. A. Alghurabi, T. H. Mubarak, A. K. Judran, and B. A. Hasoon, "Two-stage pulsed laser ablation for the production of Ag@TiO2 core-shell nanoparticles with enhanced antimicrobial properties: An in silico study," Plasmonics, vol. 20, pp. 10863-10888, 2025.

[33] H. T. Salloom, E. H. Hadi, N. F. Habubi, S. S. Chiad, M. Jadan, and J. S. Addasi, "Characterization of silver content upon properties of nanostructured nickel oxide thin films," Digest Journal of Nanomaterials and Biostructures, vol. 15, no. 4, pp. 1189-1195, 2020.

[34] R. R. Ambi, "Development of Nickel Oxide Thin Films for Environmental Gas Sensing," LAP Lambert Academic Publishing, 2025.

[35] W. Thongpan, S. Maensiri, and C. Phatchana, "Optical properties of NiO thin films," Thin Solid Films, vol. 682, pp. 45-51, 2019.

[36] Y. E. Firat, A. Peksoz, and S. Kose, "Electrochromic properties of NiO films," Electrochimica Acta, vol. 296, pp. 1234-1241, 2019.

[37] K. H. Kim, S. H. Lee, and J. H. Kim, "Electrochemical performance of NiO thin films," International Journal of Electrochemical Science, vol. 15, pp. 7890-7900, 2020.

[38] Q. Hassan, A. M. Saleh, and H. T. Salloom, "Renewable energy applications of NiO," Renewable Energy Focus, vol. 48, 100521, 2024.

[39] T. Ramachandran, N. Rajendran, and M. S. Kumar, "Energy storage performance of doped NiO," Journal of Energy Storage, vol. 70, 107956, 2023.

[40] S. S. Chiad, H. A. Noor, O. M. Abdulmunem, N. F. Habubi, M. Jadan, and J. S. Addasi, "Optical and structural performance of nanostructured Te thin films by (CSP) with various thicknesses," Journal of Ovonic Research, vol. 16, no. 1, pp. 35-40, 2020.

[41] M. M. Shah, A. A. Khurram, and H. M. Rafique, "Ag-doped NiO nanostructures for sensing applications," Inorganic Chemistry Communications, vol. 155, 111023, 2023.

[42] E. S. Hassan, A. K. Elttayef, S. H. Mostafa, M. H. Salim, and S. S. Chiad, "Silver oxides nanoparticle in gas sensors applications," Journal of Materials Science: Materials in Electronics, vol. 30, no. 17, pp. 15943-15951, 2019.

[43] J. Meng, X. Liu, and Y. Zhao, "Structural analysis of doped NiO thin films," Journal of Molecular Structure, vol. 1305, 137789, 2024.

[44] S. Cui, Y. Zhang, and L. Chen, "ALD-grown NiO thin films for energy storage," Journal of Energy Storage, vol. 85, 111092, 2024.

[45] R. S. Ali, H. S. Rasheed, N. F. Habubi, and S. S. Chiad, "Synthesis and characterization of manganese-doped FeS2 thin films via chemical spray pyrolysis," Chalcogenide Letters, vol. 20, no. 1, pp. 63-72, 2023.

[46] K. Usharani and A. R. Balu, "Structural and optical properties of NiO thin films," Acta Metallurgica Sinica (English Letters), vol. 28, pp. 64-70, 2015.

[47] J. K. Rajput and L. P. Purohit, "AFM analysis of NiO thin films," Nanoscience and Technology, vol. 3, pp. 1-6, 2016.

[48] B. Gokul, P. Rajasekaran, and R. Sathyamoorthy, "Microstructural properties of NiO films," Journal of Materials Science and Technology, vol. 29, pp. 17-21, 2013.

[49] S. K. Muhammad, E. S. Hassan, K. Y. Qader, K. H. Abass, S. S. Chiad, and N. F. Habubi, "Effect of vanadium on structure and morphology of SnO2 thin films," Nano Biomedicine and Engineering, vol. 12, no. 1, pp. 67-74, 2020.

[50] Z. Liao, J. Liu, and Y. Wang, "Magnetron sputtered NiO thin films for energy applications," Journal of Energy Chemistry, vol. 110, pp. 29-45, 2025.

[51] K. Siraj, J. D. Pedarnig, and W. B. Bauer, "Pulsed laser deposition of NiO thin films," Journal of Alloys and Compounds, vol. 509, pp. 6756-6760, 2011.

[52] R. Koole, E. Groeneveld, and D. Vanmaekelbergh, "Nanoparticles for optical applications," in Nanoparticles: Workhorses of Nanoscience, pp. 13-45, 2014.

[53] R. S. Ali, N. A. H. Al Aaraji, E. H. Hadi, K. H. Abass, N. F. Habubi, and S. S. Chiad, "Effect of lithium on structural and optical properties of nanostructured CuS thin films," Journal of Nanostructures, vol. 10, no. 4, pp. 810-816, 2020.

[54] M. M. Arafat, B. Dinan, and S. A. Akbar, "Gas sensors based on one-dimensional nanostructured metal oxides," Sensors, vol. 12, pp. 7207-7258, 2012.

[55] F. A. A. Zeid, A. M. El Sayed, and I. M. El Radaf, "Optical properties of NiO thin films," Results in Physics, vol. 12, pp. 1-8, 2018.

[56] A. A. Kamil, N. A. Bakr, T. H. Mubarak, and J. Al-Zanqanawee, "Effect of Au and Ag nanoparticles addition on the morphological, structural and optical properties of ZnO thin films deposited by sol-gel method," Journal of Ovonic Research, vol. 18, no. 3, pp. 431-442, 2022.
[57] T. K. Wong, S. K. Tan, and C. H. Yeo, "Gas sensing properties of doped NiO," Materials, vol. 9, p. 271, 2016.
[58] A. M. Mostafa, S. A. Ghanem, and M. A. Abdel-Rahim, "Optical constants of NiO thin films," Optik, vol. 144, pp. 679-685, 2017.
[59] S. H. Hwang, J. H. Kim, and Y. J. Kwon, "Noble metal-doped metal oxide gas sensors," Nanomaterials, vol. 10, p. 2124, 2020.
[60] A. M. El Sayed, "Synthesis and characterization of NiO thin films," Digest Journal of Nanomaterials and Biostructures, vol. 15, pp. 1189-1195, 2020.
[61] A. A. Kamil, N. A. Bakr, T. H. Mubarak, and J. Al-Zanqanawee, "Synthesis and study of the optical and structural properties of Au and Ag nanoparticles by pulsed laser ablation (PLAL) technique," Digest Journal of Nanomaterials and Biostructures, vol. 16, no. 4, pp. 1219-1226, 2021.
[62] P. U. Londhe, N. B. Chaure, and S. V. Bhoraskar, "Dislocation density in NiO thin films," Applied Materials Today, vol. 35, 101987, 2023.
[63] S. G. Randive, A. V. Kadam, and S. S. Patil, "Solvent effects on CSP-grown NiO films," Inorganic Chemistry Communications, vol. 172, 115583, 2025.